AJNR

Subtracted 3D CT Angiography for Evaluation of Internal Carotid Artery Aneurysms: Comparison with Conventional Digital Subtraction Angiography

S. Sakamoto, Y. Kiura, M. Shibukawa, S. Ohba, K. Arita and K. Kurisu

AJNR Am J Neuroradiol 2006, 27 (6) 1332-1337
http://www.ajnr.org/content/27/6/1332

ORIGINAL RESEARCH

Subtracted 3D CT Angiography for Evaluation of Internal Carotid Artery Aneurysms: Comparison with Conventional Digital Subtraction Angiography

S. Sakamoto
Y. Kiura
M. Shibukawa
S. Ohba
K. Arita
K. Kurisu

BACKGROUND AND PURPOSE: 3D computed tomographic angiography (3DCTA) has been used recently for the evaluation of intracerebral aneurysms, but it is difficult to use this technique to visualize aneurysms near the base of the skull because of the presence of bone. Subtracted 3DCTA could replace digital subtraction angiography (DSA) for evaluation of aneurysms near the base of the skull if the 2 methods were to give similar results. The aim of this study was to compare the evaluation of aneurysms of the internal carotid artery (ICA) near the base of the skull by subtracted 3DCTA and DSA.

METHODS: CTA and DSA were obtained in 25 patients with unruptured aneurysms of the ICA. To create subtracted 3DCTA images, we used a volume subtraction (VS) method, wherein nonenhanced volume data are subtracted from enhanced volume data. CTA and DSA were reviewed by 2 neuroradiologists who performed the detection and characterization of aneurysms of the ICA by using 2D multiplanar reformatted (MPR) and VS- and nonsubtracted (NS)-3DCTA images with volume rendering techniques.

RESULTS: DSA detected 29 aneurysms in the 25 patients. VS-3DCTA detected all 29 aneurysms in the 25 patients and was equivalent to DSA for evaluating their characteristics (location, size, and direction). NS-3DCTA detected 19 (1 cavernous, 4 ophthalmic, 1 superior hypophyseal, 7 posterior communicating, and 6 anterior choroidal artery) of these 29 aneurysms, but it could not characterize ophthalmic and superior hypophyseal artery aneurysms because they were only partly visible on NS-3DCTA because of bony structures. 2D-MPR images detected all but the small aneurysms (24 of 29 detected). VS-3DCTA and 2D-MPR could visualize all branching arteries (ophthalmic, posterior communicating, and anterior choroidal) detected by DSA, but NS-3DCTA could not visualize ophthalmic arteries because of the presence of bony structures.

CONCLUSION: VS-3DCTA can be used as an alternative to DSA for preoperative examination of aneurysms near the skull base, where it provides equivalent identification and characterization.

Conventional digital subtraction angiography (DSA) is the preferred method for detecting intracranial aneurysms because of its high spatial resolution and large field of view, but it has the disadvantage of being invasive.[1-9] As a result of recent innovations in CT scanner and workstation technology, 3D computed tomographic angiography (3DCTA) with helical scanning has become a useful, noninvasive imaging technique for evaluating cerebrovascular disease.[1,2,5-7,9,10] However, 3DCTA may be less useful than DSA for evaluation of cerebrovascular function near the base of the skull because of difficulties in separating vessels from bony structures.[1,10-12] Subtracted 3DCTA could become an alternative to DSA if the 2 methods are equivalent for the identification and characterization of aneurysms near the base of the skull.[1,10] Therefore, the aim of this study was to compare the abilities of subtracted 3DCTA and DSA to detect and characterize aneurysms of the internal carotid artery (ICA) near the base of the skull.

Methods

Between April 2002 and December 2004, 25 patients were enrolled in this study. The patients included 22 women and 3 men ranging in age from 31 to 79 years, with an average age of 59 years. The patients initially presented with nonspecific symptoms such as headache, vertigo, or tinnitus. Each patient was suspected, based on results of MR angiography (MRA), to have an unruptured aneurysm of the ICA. After MRA was performed, the patients received CTA, and, if an aneurysm was found, the patients received DSA. Thereafter, all patients with aneurysms of the ICA who received both CTA and DSA were included in this study. Informed consent for CTA and DSA was obtained from all patients.

A multisection helical CT scanner with 16 detector rows (GE Light Speed Ultra 16; GE Medical Systems, Waukesha, Wis) was used for CTA. All patients were positioned supine with the head maintained in a neutral position. A nonenhanced image (120 kV; 50 mA; gantry rotation speed, 0.5 s/rotation) was obtained by helical scanning (0.625-mm 16 collimation; table speed, 5.62 mm). Next, 75 mL of nonionic contrast medium (350 mg iodine/mL) was injected into the cubital vein with an automated injector at a flow rate of 4 mL/s. Enhanced images (120 kV and 200 mA) were scanned after 13 seconds because, in our experience, a maximum cavernous carotid enhancement was reached in approximately 15 seconds in patients without significant cardiopulmonary disease. Section-thickness (0.625 mm) images were reconstructed with an increment of 0.32 mm. The field of view (FOV) was 25 cm, and the reconstruction kernel was soft. Image postprocessing was performed by using an Advantage workstation (version 3.1; GE Medical Systems) with Virtual Place Advance (Office Azemoto, Tokyo, Japan) software. The volume-subtracted (VS)-3DCTA images were automatically generated by subtracting the non-

Received June 8, 2005; accepted after revision October 27.

From the Department of Neurosurgery, Hiroshima University Graduate School of Biomedical Sciences, Hiroshima, Japan.

Address correspondence to Shigeyuki Sakamoto, MD, Department of Neurosurgery, Hiroshima University Graduate School of Biomedical Sciences, 1-2-3 Kasumi, Minami-ku, Hiroshima 734-8551, Japan.

Table 1: Summary of 25 patients with internal carotid artery aneurysms evaluated by digital subtraction angiography (DSA) and computed tomogrAchAaphic angiography (CTA)

Patient No./ Age (y)/Sex	Location on DSA	Detection of Aneurysm			Sac Size (mm)			Neck Size (mm)			Direction of Aneurysm		Branching Artery		
		VS-CTA	NS-CTA	MPR	CTA	MPR	DSA	CTA	MPR	DSA	CTA	DSA	CTA	MPR	DSA
1/75/F	OphA				3.8	3.6	4.0	3.5	3.6	3.5	Anterosuperior	Anterosuperior	OphA	OphA	OphA
2/70/F	Cave		×		5.0	4.3	5.0	4.5	3.2	3.0	Posteromedial	Posteromedial	None	None	None
3/65/M	AchoA				4.8	5.1	4.7	4.7	2.8	3.4	Posterolateral	Posterolateral	AchoA	AchoA	AchoA
4/67/F	Cave		×		6.5	6.3	6.7	5.4	4.9	4.8	Posteromedial	Posteromedial	None	None	None
5/79/F	Cavernous				24.4	24.8	25.7	11.2	10.6	10.1	Lateral	Lateral	None	None	None
6/69/F	AchoA				6.6	6.1	6.5	3.1	2.7	2.4	Posterolateral	Posterolateral	AchoA	AchoA	AchoA
7/61/F	PcomA				5.7	5.5	5.4	2.8	2.2	2.2	Posterolateral	Posterolateral	PcomA	PcomA	PcomA
	AchoA			×	2.3		2.4	2.2	*	1.5	Posterolateral	Posterolateral	AchoA		AchoA
8/55/F	Cave		×	×	3.6		3.6	3.0	*	2.7	Inferomedial	Inferomedial	None		None
9/51/F	AchoA			×	2.0		2.0	1.5	*	1.5	Posterolateral	Posterolateral	AchoA		AchoA
10/49/M	SHA		×		3.7	4.0	3.8	3.4	3.1	3.2	Medial	Medial	None	None	None
11/62/F	OphA				9.5	10.5	10.0	5.1	4.1	4.3	Anterosuperior	Anterosuperior	OphA	OphA	OphA
	Cave		×	×	2.7	*	3.1	1.9	*	1.6	Inferomedial	Inferomedial	None		None
	Cavernous		×	×	2.6	*	3.0	2.6	*	2.0	Superior	Superior	None		None
12/55/M	PcomA				6.8	6.4	6.5	3.4	3.3	2.8	Posterolateral	Posterolateral	PcomA	PcomA	PcomA
13/59/F	Cave		×		3.5	3.6	3.3	3.1	3.0	1.4	Posteromedial	Posteromedial	None	None	None
14/38/F	SHA				5.8	6.0	5.6	3.3	2.9	2.9	Medial	Medial	None	None	None
15/48/F	Cave		×		5.0	4.8	5.2	3.5	3.0	3.2	Medial	Medial	None	None	None
16/53/F	OphA				7.5	8.0	8.3	6.7	5.7	3.9	Superior	Superior	OphA	OphA	OphA
17/62/F	PcomA				5.0	4.7	4.8	3.2	3.0	3.1	Posterolateral	Posterolateral	PcomA	PcomA	PcomA
18/64/F	PcomA				5.6	5.8	5.9	2.9	2.9	2.8	Posterior	Posterior	PcomA	PcomA	PcomA
19/73/F	PcomA				7.6	8.0	7.9	4.0	3.6	3.7	Posterolateral	Posterolateral	PcomA	PcomA	PcomA
20/65/F	AchoA				4.5	4.6	4.4	2.8	3.3	1.9	Posterolateral	Posterolateral	AchoA	AchoA	AchoA
21/60/F	AchoA				6.1	6.5	6.3	3.9	4.3	3.1	Posterolateral	Posterolateral	AchoA	AchoA	AchoA
22/58/F	PcomA				4.3	4.1	4.0	3.1	2.9	2.6	Posterolateral	Posterolateral	PcomA	PcomA	PcomA
	AchoA				6.1	6.3	6.1	4.9	4.6	4.7	Lateral	Lateral	AchoA	AchoA	AchoA
23/57/M	Cave		×		5.1	5.5	5.3	3.6	3.4	3.1	Posteromedial	Posteromedial	None	None	None
24/51/F	Cave		×		4.1	4.0	4.2	3.5	3.0	3.0	Medial	Medial	None	None	None
25/31/F	OphA				4.3	3.2	3.3	4.2	3.3	2.3	Superior	Superior	OphA	OphA	OphA

Note:—VS indicates volume subtraction; NS, nonsubtraction; MPR, 2D multiplanar reformatted imaging; OphA, ophthalmic artery; AchoA, anterior choroidal artery; SHA, superior hypophyseal artery.

enhanced volume data from the enhanced volume data. VS-3DCTA and nonsubtracted (NS)-3DCTA images with volume-rendering techniques, and 2D-multiplanar reformatted (MPR) images were created. The total examination time for CTA was approximately 8 minutes per case.

Standard DSA was performed with the use of a biplane DSA unit (Neurostar, Siemens, Erlangen, Germany) with a matrix resolution of 1024 × 1024 pixels. DSA was performed with bilateral selective common carotid artery injections, and either unilateral or bilateral vertebral artery injections, as necessary. For each imaged vessel, at least 3 projections, including anteroposterior, lateral, and oblique views, were obtained by manual injection of 6 to 8 mL of nonionic contrast medium. The total amount of contrast medium used was 80 to 100 mL.

VS-3DCTA and NS-3DCTA images with volume-rendering techniques, 2D-MPR images, and DSA images were interpreted by 2 neuroradiologists with no previous knowledge of the existence of intracranial aneurysms. 2D-MPR images were viewed in cine mode with axial, sagittal, and coronal views. The neuroradiologists evaluated the presence and characteristics (location, size of sac and neck, and direction) of the aneurysms and branching arteries from the aneurysms. The location of the aneurysm was classified as follows: anterior choroidal artery (AchoA) aneurysms included those with necks arising at the junction of the AchoA and the ICA; posterior communicating artery (PcomA) aneurysms included those with necks arising at the junction of the PcomA and the ICA; superior hypophyseal artery (SHA) aneurysms included those located at the medial or inferomedial wall of the ophthalmic segment of the ICA[13]; ophthalmic artery (OphA) aneurysms included those with necks arising at the junction of the OphA and the ICA; carotid cave aneurysms included those located in medial infraophthalmic and supracavernous regions[14]; and cavernous aneurysms included those with necks arising from the cavernous segment of the ICA. The size of the aneurysm sac was defined as its maximum diameter. The characterization of aneurysms was confirmed by DSA or surgical evaluation.

Results

Table 1 summarizes the results of this study. A total of 29 aneurysms was detected by DSA in the 25 patients. Twenty-two patients had a single aneurysm, 2 patients had 2 aneurysms, and 1 patient had 3 aneurysms (Fig 1). Of the 29 aneurysms, 7 (24.1%) were AchoA, 6 (20.6%) were PcomA, 2 (6.9%) were SHA, 4 (13.8%) were OphA, 8 (27.6%) were carotid cave, and 2 (6.9%) were cavernous (Tables 1 and 2).

The detection and characteristics including the location, size, and direction of the aneurysms on CTA are summarized in Table 2. VS-3DCTA detected all 29 (100%) of the aneurysms in the 25 patients. NS-3DCTA detected only 19 (65%) of these 29 aneurysms. Of the aneurysms detected, the size and direction of OphA, SHA, and carotid cave aneurysms could not be evaluated because they were only partly visible on NS-3DCTA because of the presence of bony structures. Of the 10 aneurysms not detected on NS-3DCTA, 8 were carotid cave, 1 was cavernous, and 1 was SHA (Figs 1 and 2). 2D-MPR images

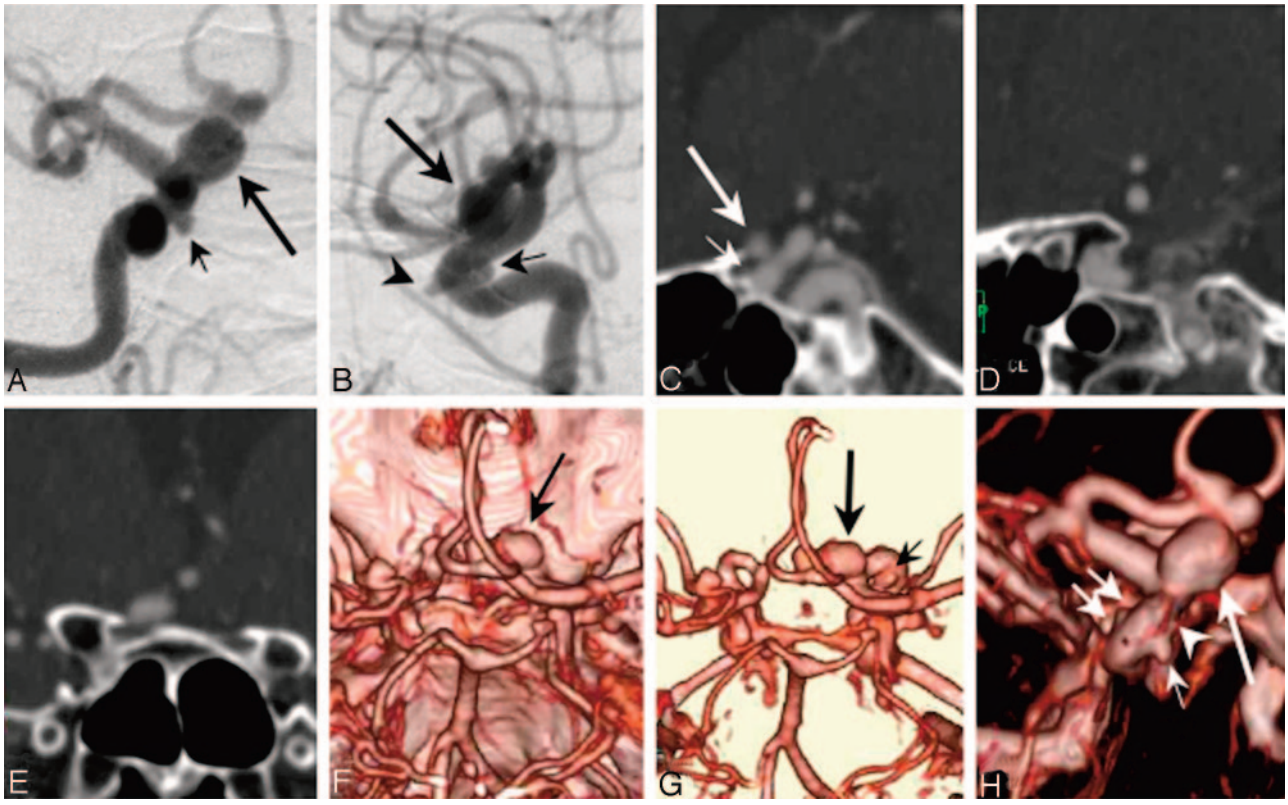

Fig 1. Case 11: Patient with 3 ophthalmic artery (OphA), 1 carotid cave, and 1 cavernous aneurysm. *A,* Intraarterial angiogram, oblique view, showing the right OphA aneurysm (*long arrow*) and the right carotid cave aneurysm (*short arrow*).

B, Intraarterial angiogram, lateral view, showing the right OphA aneurysm (*long arrow*), the right carotid cave aneurysm (*arrowhead*), and the right cavernous aneurysm (*short arrow*).

C, Multiplanar reformatted (MPR) image, sagittal view, showing the right OphA aneurysm (*long arrow*) and OphA branching at the aneurysm neck (*short arrow*).

D, MPR image, sagittal view, which did not clearly visualize the right cavernous aneurysm.

E, MPR image, sagittal view, which did not clearly visualize the right carotid cave aneurysm.

F, Nonsubtracted (NS) 3D computed tomographic angiography (3DCTA), superior view, showing the right OphA aneurysm (*arrow*), but the right carotid cave and cavernous aneurysms were not visualized.

G, Volume-subtracted (VS)-3DCTA, superior view, clearly showing the right OphA (*long arrow*) and the right cavernous aneurysm (*short arrow*).

H, VS-3DCTA, oblique view, clearly showing the right OphA aneurysm (*long arrow*), the right carotid cave aneurysm (*short arrow*), the right cavernous aneurysm (*double arrows*), and OphA branching at aneurysm neck (*arrowhead*).

Table 2: Detection and location of 29 aneurysms

	Detection of Aneurysms			
Location of Aneurysm	DSA	VS-CTA	NS-CTA	MPR
Anterior choroidal artery	7	7	7	5
Posterior communicating artery	6	6	6	6
Superior hypohyseal artery	2	2	1	2
Ophthalmic artery	4	4	4	4
Carotid cave	8	8	0	6
Carotid cavernous	2	2	1	1
Total	29	29	19	24

Note:—DSA indicates digital subtraction angiography; VS-CTA, volume subtraction computed tomographic angiography; NS-CTA, nonsubtraction computed tomographic angiography; MPR, 2D multiplaner reformatted imaging.

detected 24 (82%) of these 29 aneurysms. Of the 5 aneurysms not detected on 2D-MPR, 2 were carotid cave, 2 were AchoA, and 1 was cavernous of less than 3 mm (Fig 1). With respect to the detection of ICA aneurysms, VS-3DCTA and DSA were equivalent; 2D-MPR images were slightly worse than DSA for small aneurysms; and NS-DCTA was worse than DSA for carotid cave, cavernous, and SHA aneurysms. In addition, 3DCTA and 2D-MPR were as effective as DSA for visualizing infundibular widening of the PcomA (Fig 2).

The size of the aneurysm sac revealed by DSA ranged from 2.0 to 25.7 mm, with a mean size of 5.7 mm. According to DSA measurements, 2 (6.8%) of the aneurysms were <3 mm, 13 (44.8%) were 3 to 5 mm, 13 (44.8%) were 5.1 to 10 mm, and 1 (3.4%) was >10 mm. The size of aneurysm neck revealed by DSA ranged from 1.4 to 10.1 mm, with a mean size of 3.1 mm. The size of aneurysm sac determined by VS- and/or NS-3DCTA ranged from 2.0 to 24.4 mm, with a mean size of 5.7 mm. According VS- and/or NS-3DCTA measurements, 4 (13.8%) of the aneurysms were <3 mm, 12 (41.3%) were 3 to 5 mm, 12 (41.3%) were 5.1 to 10 mm, and 1 (3.4%) was >10 mm. The size of aneurysm neck revealed by 3DCTA ranged from 1.5 to 11.2 mm, with a mean size of 3.8 mm. Excluding the 5 aneurysms that were not detected, the size of aneurysm sac revealed by 2D-MPR ranged from 3.2 to 24.8 mm, with a mean size of 6.3 mm. By 2D-MPR, the aneurysms of less than 3 mm were not detected; of those detected, 10 (41.7%) were 3 to 5 mm, 12 (50.0%) were 5.1 to 10 mm, and 2 (8.3%) were >10 mm. The size of aneurysm neck revealed by 2D-MPR ranged from 2.2 to 10.6 mm, with a mean size of 3.7 mm.

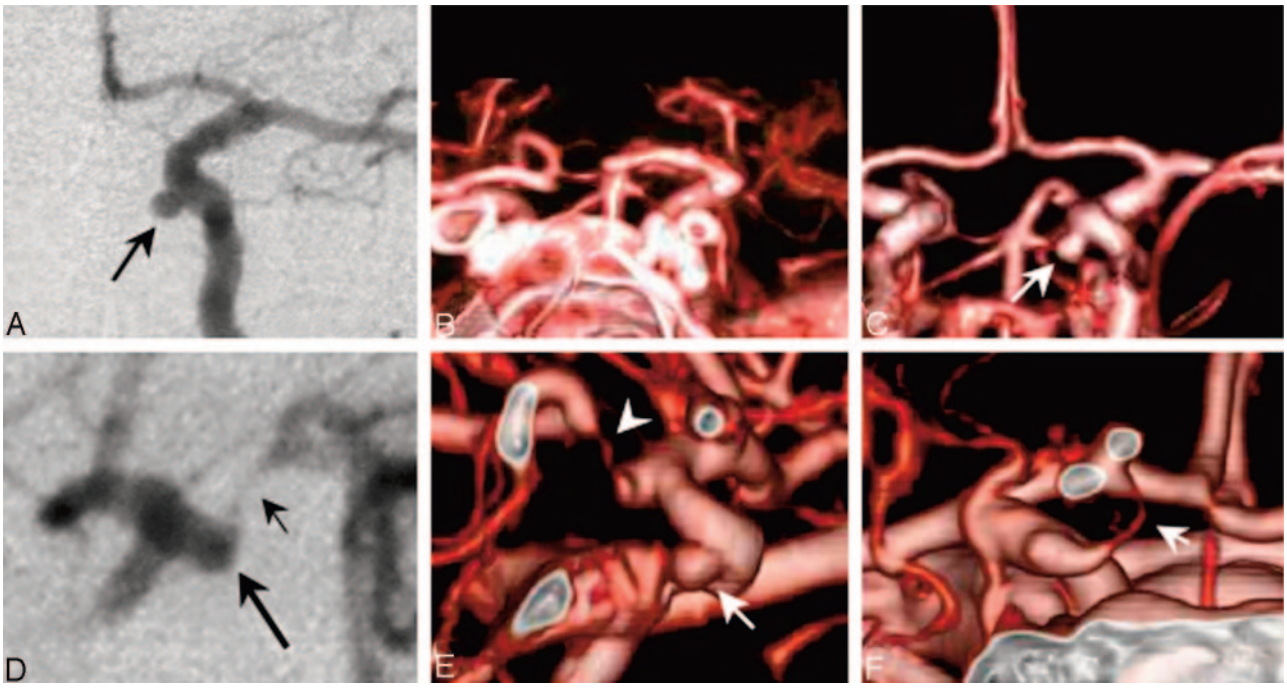

Fig 2. Case 8: Patient with 1 carotid cave aneurysm and infundibular widening of the posterior communicating artery (PcomA). *A,* Intraarterial angiogram, anteroposterior view, showing the left carotid cave aneurysm in the inferomedial direction (*arrow*).

B, Nonsubtracted (NS) 3D computed tomographic angiography (3DCTA), anteroposterior view, which did not show the left carotid cave aneurysm.

C, Volume subtraction (VS)-3DCTA, anteroposterior view, clearly showing the left carotid cave aneurysm with inferomedial direction (*arrow*).

D, Intra-arterial angiogram, lateral view, showing an infundibular widening (*long arrow*) of the left PcomA and a PcomA (*short arrow*) originating from the top of the infundibular widening.

E, VS-3DCTA, medial view, showing the left carotid cave aneurysm in the inferomedial direction (*arrow*) and the PcomA (*arrowhead*) originating from the top of the infundibular widening.

F, NS-3DCTA, posterior view, showing the infundibular widening of the left PcomA and the PcomA (*arrow*) originating from the top of the infundibular widening.

Table 3: Sac size of 29 aneurysms

Size of Aneurysm (mm)	DSA	CTA
<3	2	4
3–5	13	12
5.1–10	13	12
>10	1	1
Total	29	29

Note:—DSA indicates digital subtraction angiography; CTA, computed tomographic angiography.

Table 4: Branching artery from 29 aneurysms

Branching Artery	DSA	CTA	MPR
Anterior choroidal artery	7	7	6
Posterior communicating artery	6	6	6
Ophthalmic artery	4	4	4
Total	17	17	16

Note:—DSA indicates digital subtraction angiography; CTA, computed tomographic angiography; MPR, 2D multiplanar reformatted imaging.

These results showed that the size of the aneurysm sac measured by 3D images and 2D images corresponded well to the size measured by DSA, but the size of the aneurysm neck measured by 3D images tends to be larger than that measured by DSA (Tables 1 and 3).

DSA and 3DCTA showed similar results for the directions of aneurysms (Table 1). The direction of the ICA aneurysms was as follows: of 7 AchoA aneurysms, projection was posterolateral for 6 and lateral for 1; of 6 PcomA aneurysms, projection was posterolateral for 5 and posterior for 1; for the 2 SHA aneurysms, projection of both was medial; of 4 OphA aneurysms, projection was anterosuperior for 2 and superior for 2; of 8 carotid cave aneurysms, projection was posteromedial for 4, inferomedial for 2, and medial for 2; and of 2 cavernous aneurysms, projection was superior for 1, and lateral for 1.

DSA revealed a total of 17 branching arteries from aneurysms. Of these, 7 were AchoA, 6 PcomA, and 4 OphA (Tables 1 and 4). VS-3DCTA also detected 17 (100%) of the 17 branching arteries at aneurysm necks. 2D-MPR images detected the 16 branching arteries except from 1 AchoA aneurysm not detected on MPR. These results showed that 3DCTA and 2D-MPR were also equivalent to DSA for the detection of branching arteries from aneurysms (Fig 3).

Discussion

3DCTA has been an important tool for noninvasive evaluation of the vasculature, and there have been numerous reports on its accuracy and utility for detecting intracranial aneurysms.[1-9] Single-section CTA has a high sensitivity for aneurysms larger than 3 mm[6,15] and has been reported to provide 67% to 100% sensitivity and 92% to 100% specificity for the detection of intracranial aneurysms.[5,9,15,16] Furthermore, in a study of 50 patients, Wintermark et al[15] found that multisection CTA provided 95% sensitivity and 95% specificity for the detection of intracranial aneurysms. In a 35-patient study of multisection CTA, Jayaraman et al[3] found high sensitivity and specificity for the detection of intracranial aneurysms, including small aneurysms. However, aneurysms in the base of the skull near the circle of Willis might not appear clearly on conventional NS-3DCTA because of the difficulty in visually separating vessels from bone. Therefore, conventional NS-3DCTA

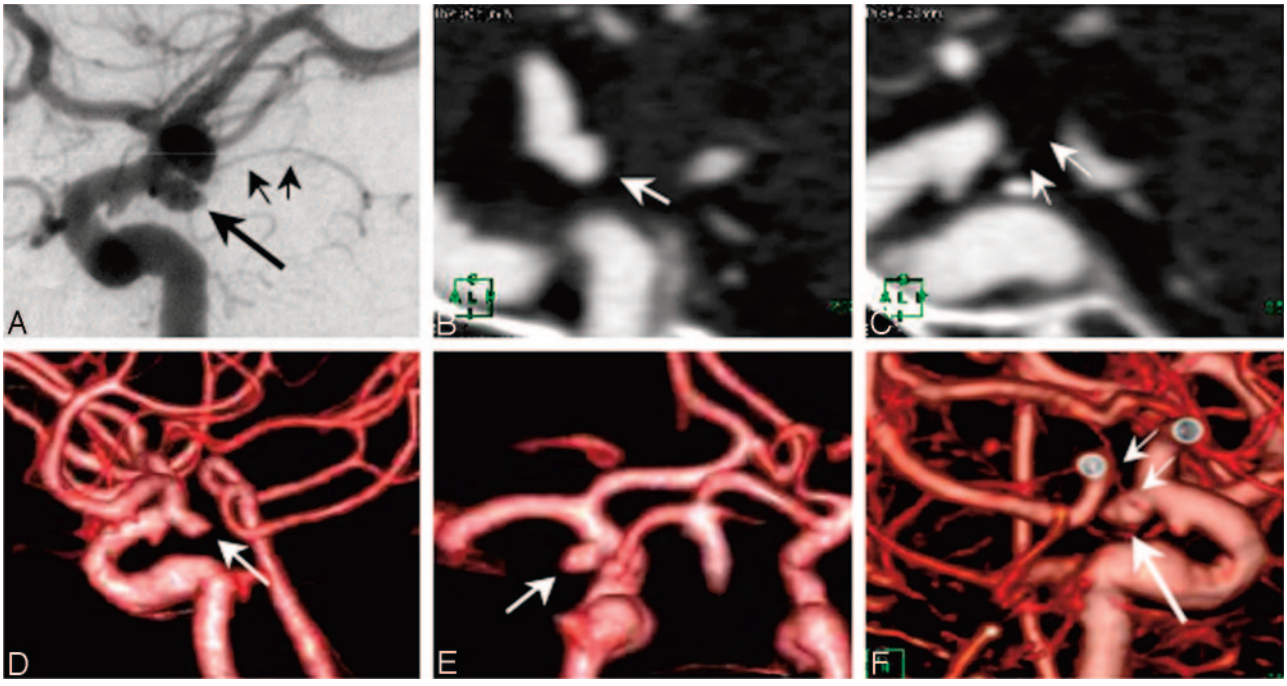

Fig 3. Case 20: Patient with 1 anterior choroidal artery (AchoA) aneurysm. *A,* Intra-arterial angiogram, lateral view, showing the left AchoA aneurysm (*long arrow*) originating at the junction of the AchoA (*short arrows*) and the internal carotid artery (ICA).

B, Multiplanar reformatted (MPR) image, sagittal view, showing the left AchoA aneurysm (*arrow*).

C, MPR image, sagittal view, showing AchoA branching at aneurysm neck (*arrows*).

D, Volume subtracted (VS)-3D computed tomographic angiography (3DCTA), lateral view, showing the left AchoA aneurysm (*arrow*).

E, VS-3DCTA, posterior view, showing the left AchoA aneurysm with a posterolateral direction (*arrow*).

F, VS-3DCTA, medial view, clearly showing the left AchoA aneurysm (*long arrow*) and AchoA branching at the aneurysm neck (*short arrows*).

had been less useful than DSA for detecting aneurysms near the base of the skull.[1,10-12]

A few subtraction methods have been studied for 3DCTA.[1,2,10] In a study of 30 patients, Jayakrishnan et al[2] found that subtraction 3DCTA in conjunction with a simple head-restraining device and a slight modification of the image processing software is more effective than conventional CTA in detecting vascular disease in intracranial and extracranial arteries. In another study of 36 patients, Imakita et al[1] showed that subtraction CTA with controlled-orbit helical scanning is superior to conventional CTA for detecting aneurysms adjacent to bone. Sakamoto et al[10] reported a case of carotid cave aneurysm that was detected by VS-3DCTA but not by NS-3DCTA. In our study, although 10 (38%) of the 29 ICA aneurysms were near bone and not detected by NS-3DCTA, all 29 aneurysms were clearly found by VS-3DCTA. Therefore, subtracted 3DCTA seems to be superior to conventional NS-3DCTA for the detection of aneurysms of the ICA adjacent to bone.[1,2,10]

Although DSA has been considered the preferred method for the diagnosis of intracranial aneurysms, it is invasive, potentially time-consuming, operator-dependent, and carries a 4% risk of complications and 1% rate of persistent neurologic deficit.[5,8] The radiation dose in CTA has been estimated to be less than that of DSA.[17] If VS-3DCTA is as effective as DSA for detecting ICA aneurysms adjacent to bone, VS-3DCTA may be a better choice because it is easier to perform and is noninvasive. To our knowledge, 2 studies so far have compared subtracted 3DCTA and DSA.[1,18] Imakita et al[1] reported in a study of 32 patients with a total of 46 aneurysms that detection by subtraction 3DCTA was as good as or better than detection by DSA. Based on these results, they concluded that subtraction 3DCTA was effective for the detection of aneurysms adjacent to bone.[1] Abrahams et al[18] also reported that a subtracted 3DCTA method and DSA both detected a total of 8 aneurysms in 6 patients. Together, these findings suggest that subtracted 3DCTA is equivalent to DSA for detecting aneurysms of the ICA adjacent to bone.

Multisection CTA allows a precise evaluation of the size and direction of aneurysms, and it has a practical detection limit of 2 mm.[3,15] In the current study, the size and direction of aneurysms on VS-3DCTA correlated well with the DSA findings. Thus, subtracted 3DCTA seems to be equivalent to DSA for evaluation of the morphology of aneurysms with size and direction. On the other hand, it is important to evaluate branching arteries from aneurysms for the planning of treatments. The branching arteries from ICA aneurysms are OphA, PcomA, SHA, and AchoA. The SHA and AchoA are considerably smaller than 0.3 and 0.5 mm, respectively.[13,17,19] Even DSA with high spatial resolution (0.3-mm resolution) does not usually show the SHA.[13,19] The current resolution of CTA is approximately 0.4 to 0.5 mm, and the through-plane resolution is 1 mm.[17] Therefore, although CTA may be able to reveal a portion of small arteries such as the AchoA, it may not be effective for visualizing the long parts of them.[5,16,17] For surgical treatment, especially endovascular treatment, it is very important to identify branching arteries at the neck of the aneurysm.[16] Of a total of 17 branching arteries from aneu-

rysms detected by DSA, all 17 were revealed by 3DCTA. In this study, CTA was performed by using a multidetector row scanner with 16 detector rows, a 0.625-mm section thickness, and a FOV of 25 cm. If we used an FOV of 18 cm, which is generally large enough to include the entire head, we might have improved the resolution to a pixel size of 0.35 mm and might have been able to more clearly visualize very small arteries.[17,20]

Compared with CTA and DSA, MRA has the advantage of not exposing the patient to radiation and not requiring an iodinated contrast agent. However, MRA generally has a lower resolution than both CTA and DSA because of a smaller matrix size, an increased phase dispersion, a large FOV, and the occurrence of patient motion artifacts as a result of relatively long scan times.[5,17]

The 3D images were most useful for detecting and characterizing intradural lesions that are obvious when viewed in a 3D environment but not when viewed in a 2D mode.[20] Villablanca et al[20] evaluated the detection and characterization of small aneurysms by using 2D- and 3DCTA. They reported that when using only 3D images, an aneurysm was discovered in 10% of the cases, with subsequent lesion confirmation and quantitation made by using 2D sections. In our study, NS-3DCTA combined with 2D-MPR is almost as effective as VS-3DCTA for evaluating aneurysms near the base of the skull. Although we used a low amperage for the mask CT, it was still more radiation than used for 3DCTA without subtraction. However, the most important role of the 3D technique is to help clarify the shape of the aneurysmal sac and neck and to determine the spatial relationship between the sac to the surrounding branches. Therefore, VS-3DCTA should be selected in place of NS-3DCTA plus 2D-MPR for preoperative examination of aneurysms near the skull base, especially cavernous, carotid cave, and OphA types.

In conclusion, this study showed that VS-3DCTA is more effective than DSA for evaluating ICA aneurysms near the base of the skull. For detection and characterization of the aneurysms, including further branching arteries at the aneurysm necks, 3DCTA was equal to DSA. This is the first study to show that 3DCTA is equal to DSA for evaluation of aneurysms near the base of the skull. These results and previous reports indicate that 3DCTA is a good alternative to DSA for evaluation of intracranial aneurysms near the base of the skull.[3,20]

References

1. Imakita S, Onishi Y, Hashimoto T, et al. **Subtraction CT angiography with controlled-orbit helical scanning for detection of intracranial aneurysms.** *AJNR Am J Neuroradiol* 1998;19:291–95
2. Jayakrishnan VK, White PM, Aitken D, et al. **Subtraction helical CT angiography of intra- and extracranial vessels: technical considerations and preliminary experience.** *AJNR Am J Neuroradiol* 2003;24:451–55
3. Jayaraman MV, Mayo-Smith WW, Tung GA, et al. **Detection of intracranial aneurysms: multi-detector row CT angiography compared with DSA.** *Radiology* 2004;230:510–18
4. Kangasniemi M, Makela T, Koskinen S, et al. **Detection of intracranial aneurysms with two-dimensional and three-dimensional multislice helical computed tomographic angiography.** *Neurosurgery* 2004;54:336–40
5. Karamessini MT, Kagadis GC, Petsas T, et al. **CT angiography with three-dimensional techniques for the early diagnosis of intracranial aneurysms. Comparison with intra-arterial DSA and the surgical findings.** *Eur J Radiol* 2004; 49:212–23
6. Korogi Y, Takahashi M, Katada K, et al. **Intracranial aneurysms: detection with three-dimensional CT angiography with volume rendering–comparison with conventional angiographic and surgical findings.** *Radiology* 1999;211: 497–506
7. Ogawa T, Okudera T, Noguchi K, et al. **Cerebral aneurysms: evaluation with three-dimensional CT angiography.** *AJNR Am J Neuroradiol* 1996;17:447–54
8. Waugh JR, Sacharias N. **Arteriographic complications in the DSA era.** *Radiology* 1992;182:243–46
9. White PM, Wardlaw JM, Easton V. **Can noninvasive imaging accurately depict intracranial aneurysms? A systematic review.** *Radiology* 2000;217:361–70
10. Sakamoto S, Kiura Y, Ohba S, et al. **Volume subtraction three-dimensional CT angiography for cerebrovascular disease: report of two cases.** *Hiroshima J Med Sci* 2005;53:83–86
11. Anderson GB, Steinke DE, Petruk KC, et al. **Computed tomographic angiography versus digital subtraction angiography for the diagnosis and early treatment of ruptured intracranial aneurysms.** *Neurosurgery* 1999;45:1315–20
12. Schwartz RB, Tice HM, Hooten SM, et al. **Evaluation of cerebral aneurysms with helical CT: correlation with conventional angiography and MR angiography.** *Radiology* 1994;192:717–22
13. Tanaka Y, Hongo K, Tada T, et al. **Radiometric analysis of paraclinoid carotid artery aneurysms.** *J Neurosurg* 2002;96:649–53
14. Kobayashi S, Kyoshima K, Gibo H, et al. **Carotid cave aneurysms of the internal carotid artery.** *J Neurosurg* 1989;70:216–21
15. Wintermark M, Uske A, Chalaron M, et al. **Multislice computerized tomography angiography in the evaluation of intracranial aneurysms: a comparison with intraarterial digital subtraction angiography.** *J Neurosurg* 2003;98: 828–36
16. Matsumoto M, Sato M, Nakano M, et al. **Three-dimensional computerized tomography angiography-guided surgery of acutely ruptured cerebral aneurysms.** *J Neurosurg* 2001;94:718–27
17. Villablanca JP, Martin N, Jahan R, et al. **Volume-rendered helical computerized tomography angiography in the detection and characterization of intracranial aneurysms.** *J Neurosurg* 2000;93:254–64
18. Abrahams JM, Saha PK, Hurst RW, et al. **Three-dimensional bone-free rendering of the cerebral circulation by use of computed tomographic angiography and fuzzy connectedness.** *Neurosurgery* 2002;51:264–68
19. Krisht AF, Barrow DL, Barnett DW, et al. **The microsurgical anatomy of the superior hypophyseal artery.** *Neurosurgery* 1994;35:899–903
20. Villablanca JP, Jahan R, Hooshi P, et al. **Detection and characterization of very small cerebral aneurysms by using 2D and 3D helical CT angiography.** *AJNR Am J Neuroradiol* 2002;23:1187–98